Effect of Charge Asymmetry on Adsorption and Phase Separation of Polyampholytes on Silica and Cellulose Surfaces

Junlong Song,[†,⊥] Takashi Yamagushi,[‡] Deusanilde J. Silva,[§] Martin A. Hubbe,[†] and Orlando J. Rojas*[,†,∥]

Department of Forest Biomaterials, North Carolina State University, Campus Box 8005, Raleigh, North Carolina 27695-8005, Nippon Paper Industries Co., Ltd., 1-2-2, Hitotsubashi, Chiyoda-ku, Tokyo 100-0003, Japan, Department of Chemical Engineering, Polytechnic School of São Paulo University, SP, Brazil, and Department of Forest Products Technology, Faculty of Chemistry and Materials Sciences, Helsinki University of Technology, P.O. Box 3320, FIN-02015 TKK, Espoo, Finland

Received: September 18, 2009; Revised Manuscript Received: October 28, 2009

The relation between the properties of polyampholytes in aqueous solution and their adsorption behaviors on silica and cellulose surfaces was investigated. Four polyampholytes carrying different charge densities but with the same nominal ratio of positive to negative segments and two structurally similar polyelectrolytes (a polyacid and a polybase) were investigated by using quartz crystal microgravimetry using silica-coated and cellulose-coated quartz resonators. Time-resolved mass and rigidity (or viscoelasticity) of the adsorbed layer was determined from the shifts in frequency (Δf) and energy dissipation (ΔD) of the respective resonator. Therefore, elucidation of the dynamics and extent of adsorption, as well as the conformational changes of the adsorbed macromolecules, were possible. The charge properties of the solid surface played a crucial role in the adsorption of the studied polyampholytes, which was explained by the capability of the surface to polarize the polyampholyte at the interface. Under the same experimental conditions, the polyampholytes had a higher nominal charge density phase-separated near the interface, producing a soft, dissipative, and loosely bound layer. In the case of cellulose substrates, where adsorption was limited, electrostatic and polarization effects were concluded to be less significant.

Introduction

Polyampholytes are charged macromolecules carrying both acidic and basic groups. Under appropriate conditions, these macromolecules dissociate in aqueous solution, producing ionic groups on the polymer chains and the respective counterions in solution. If the ionic groups on the polymer chain are weak acids or bases, then the net charge of the polyampholyte can be changed by varying the pH of the aqueous medium. Close to the isoelectric pH, they exhibit a small net charge and display the characteristic properties of polyampholytes.[1−10] For example, the degree of extension of polyampholytes close to the charge-balanced state tends to increase with increasing salt concentration. At the isoelectric pH, the amounts of positive and negative charges on the polyion are balanced (charge symmetry), giving a net charge of zero. However, under conditions of pH where there is high charge asymmetry (well above or below the isoelectric point), polyampholytes behave similarly to simple polyelectrolytes.

Due to the unique properties of polyampholytes, they have found promise in applications involving wetting, lubrication, adhesion, and other phenomena.[11−15] Polyampholytes are used to control the colloidal stability of dispersions in wastewater treatment and other applications involving aqueous mixtures.[12,16] It has been demonstrated that polyampholytes provide superior strength improvements for paper manufacture, compared to the addition of simple polyelectrolytes.[14,15,17−20] Finally, synthetic polyampholytes have been reported as electrical analogues of proteins.[1,21] Therefore, understanding the behavior of polyampholytes with defined charge balance and structure can be expected to also shed light on biomacromolecular adsorption at interfaces.

There is a need for characterizing polyampholyte adsorption that will lead to new functional materials and performance. Despite the existence of several theoretical and computational reports on their behaviors at solid interfaces,[2,3,6,7,10,22−26] experimental data to critically test the proposed theories and to directly allow the elucidation of the complex polyampholyte adsorption are still lacking.[16,27]

Several methods are available to study polymer adsorption on planar surfaces. These include radio labeling,[28] reflectance FTIR,[29] in situ ellipsometry,[30] and surface plasmon resonance.[31−35] However, the main technique employed in our experiments consisted of quartz crystal microgravimetry. The mechanical oscillatory nature of quartz resonators enabled the measurement of unique properties such as the viscoelasticity of adsorbed polymer layers, in addition to the mass uptake on the solid surface.[36−39]

A series of experiments with synthetic, random polyampholytes having increasing total nominal charge densities (at a constant ratio of cationic to anionic monomeric groups and molecular mass) was conducted. Silica and cellulose carrying negative electrostatic charges (but with different densities) were used as substrates for adsorption. The effect of the pH of the adsorbing polymer solution (and thus the polymer charge

* Corresponding author. Tel.: +1-919-513-7494. Fax: +1-919-515 6302. E-mail: ojrojas@ncsu.edu.
[†] North Carolina State University.
[‡] Nippon Paper Industries Co., Ltd.
[§] Polytechnic School of São Paulo University.
[∥] Helsinki University of Technology.
[⊥] Present address: College of Light Industry, Nanjing Forestry University, Nanjing, Jiangsu, 210037 China.

10.1021/jp909047t
Published on Web 11/19/2009

TABLE 1: Acrylamide-Based Polyampholytes (PAmp2, 4, 8, and 16) and Simple Polyelectrolytes (Cat and An)[a]

sample	polymer type	cationic groups (mol %)	cationic groups, NMR (mol %)	anionic groups (mol %)	anionic groups, NMR (mol %)	viscosity[c] (mPa•s)	M_w[d] (10^6 Da)
PAmp2	amphoteric	2.5	2.6	2	2.4	5300	2.95
PAmp4	amphoteric	5	5	4	4.4	4900	2.85
PAmp8	amphoteric	10	9.5	8	9.6	4000	2.90
PAmp16	amphoteric	20	18	16	16.8	2400	2.93
Cat	cationic	5	5	0	(1.2)	3600	2.98
An	anionic	0.5	0.5	4	3.6	5300	3.23

[a] Note that in the case of the polyampholytes the % mol ratio for cationic-to-anionic groups was kept constant at 5:4, and the molecular weight was approximately the same for all polymer samples ([b]). [b] Note that in the text the charge density of the polyampholyte samples is referred to as "nominal charge density" to indicate the presence of functional groups that can become charged, depending on the solution conditions (pH, etc.). [c] Solution with 15% polymer measured at 25 °C and 100 s^{-1}. [d] SEC-LALLS-VIS (TDA-302, Viscotek).

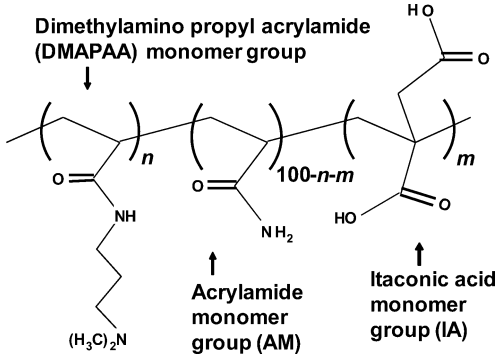

Figure 1. Molecular structures of monomers (DMAPAA, IA, and AM) in random polyampholytes prepared by free-radical polymerization. The subscripts "*n*" and "*m*" stand for the number percent of monomer units in random positions.

asymmetry) on the dynamics and extent of adsorption was investigated. The main aim of this research was to clarify the relationship between the charged nature of the polymers and the adsorption and conformation of the respective adsorbed layers. An additional question to be elucidated was whether the relationship between the bulk and the surface behavior of polyampholytes is comparable to those of neutral polymers as well as simple polyelectrolytes.

Experimental Section

Polyampholytes and Simple Polyelectrolytes. Polyampholyte and polyelectrolyte samples were prepared by free-radical polymerization, giving a final content of charged monomers as indicated in Table 1. A representative structure of the random, amphoteric terpolymers used is shown in Figure 1. Their preparation and characterization was addressed in detail in ref 20. The cationic monomer was *N*-[3-(*N*′,*N*′-dimethylamino)propyl]acrylamide (DMAPAA), a tertiary amine. The anionic monomer was a dicarboxylic acid, methylene butanedioic acid, also known as itaconic acid (IA). In each case, the balance amount of neutral acrylamide (AM) monomer was added to comprise 100% on a molar basis. The percentages of each monomer and molecular weight for the four polyampholytes and the cationic and anionic samples along with experimental values obtained via NMR are summarized in Table 1, which also lists other physical characteristics. All the polymers were expected to be random with regard to the distribution of different monomers in the macromolecular structure, but no attempt was made to confirm this characteristic.

Inorganic chemicals, including hydrochloric acid, sodium hydroxide, sodium chloride, and sodium sulfate were of reagent grade and acquired from Aldrich. All experiments were performed with deionized water from an ion-exchange system (Pureflow, Inc.) followed by a Milli-Q Gradient unit (resistivity >18 MΩ).

The pH at the isoelectric point (IEP) for PAmp16 was found to be 7.3 at 10 mM salt concentration, as determined by polyelectrolyte titration with polyvinyl sulfate (potassium salt) to a neutral streaming current end point using a Mütek PCD-04 charge analyzer from BTG. The IEPs for the other polyampholyte samples (PAmp 2, 4, 8) were all close to neutral pH. Solution viscosities were obtained with a Brookfield model B8L viscometer (Tokimec, Inc.) at approximately 15% solids at 25 °C. Molecular weight was obtained via multiangle light scattering with a SEC-LALLS-VIS (TDA-302, Viscotek) (see Table 1).

A DAWN laser photometer and an OPTILAB interferometric refractometer of Wyatt Technology Corporation were employed to measure the radius of gyration of PAmp4 under three conditions of pH (4, 7, and 10). These acidic, neutral, and basic conditions were used to produce Zimm plots from the static light scattering data. The radius of gyration (R_g) of PAmp4 in aqueous solution at pH 4, 7, and 10 was 95 ± 6, 69 ± 7, and 182 ± 36 nm, respectively. The hydrodynamic diameter and turbidity of the polymer with the highest charge density, PAmp16, were measured as a function of pH using a dynamic light scattering system (Beckman Coulter N4 Plus) with a 10 mW Helium−Neon laser ($\lambda = 632.8$ nm) as a light source. The measurements were performed at a PAmp16 concentration of 336 mg/L in 10 mM NaCl solution. A maximum in the hydrodynamic radius was observed at around the IEP, while the turbidity reached relative maxima at values of pH slightly below or above the IEP. This could be interpreted as being due to the association between macromolecules that formed aggregates with the pH approaching the IEP since the electrostatic repulsion is expected to be limited at this point. Far from the IEP and because of the attraction by local positive and negative groups, the polyampholyte molecules contracted and assembled into coils. Also, the viscosity of the polymer solutions decreased with increased polymer charge density, as observed from viscosity data reported in Table 1, which is consistent with the characteristic tendency of polyampholytes to contract when they are less charged.

The relation between pH and the macromolecular size was consistent with the theoretical work of several authors, who indicated that polyampholytes contract into coiled conformations in the vicinity of their IEP but expand by the effect of the charge asymmetry at extreme pH conditions.[1,3,22]

Silica and Cellulose Substrates. The substrates used in this investigation consisted of AT-cut quartz sensors coated with gold (fundamental frequency of 5 MHz) for use in a quartz crystal microgravimetry. These sensors were also coated with

silica or cellulose layers. Silica-coated crystals, available commercially from Q-Sense (Gothenburg, Sweden), were cleaned by immersion in 2% sodium dodecyl sulfate solution for at least 30 min, followed by double rinsing with Milli-Q grade water and drying with nitrogen. Just before use, the silica-coated crystals were treated with UV-ozone for 10 min to oxidize impurities and to activate silanol groups on the surface. The type and magnitude of the charges on the silica surfaces depended on their conditioning, the pH of the surrounding aqueous medium, and the background electrolyte (type and concentration). For example, Radtchenko et al. determined a charge density of colloidal silica probes of −0.4 and −2 mC/m^2 at pH 4 and 9.5, respectively, by using AFM force measurements against flat silica.[40]

Cellulose thin films were produced from microcrystalline cellulose (Avicel purchased from Fisher). The films were spin coated from NMMO solution on the silica-coated sensors. The protocol followed in the manufacture of the cellulose films, and their quality has been addressed in detail elsewhere.[41−43] Comparatively, the charge density of cellulose is much lower than that of silica.[40,44,45] For example, surface charges of −0.21 and −0.80 mC/m^2 at pH 4 and 9.5, respectively, were obtained by fitting AFM force profiles to the DLVO equation in the case of cellulose films spin-coated from LiCl/*N*,*N*-dimethylacetamide solution.[40]

Quartz Crystal Microbalance Measurements. Adsorption experiments with the polyampholytes and the simple polyelectrolytes were conducted on a quartz crystal microbalance (QCM) with dissipation monitoring, QCM-D Q300 model (Q-Sense, Gothenburg, Sweden), while experiments on the effect of pH on adsorption were conducted with a QCM-D E4 model (Q-Sense, Gothenburg, Sweden) run under continuous flow configuration. The principles of this technique can be found in refs 38, 39, and 46. In the case of adsorbed rigid layers, the Sauerbrey equation that relates the change in the mass of the sensor (Δm) and the recorded change in its oscillation frequency (Δf) can be applied

$$\Delta m = c\frac{\Delta f_n}{n}$$

where n is the overtone number (n = 1, 3, 5, and 7) and c is a constant representing the mass sensitivity at 5 MHz. For the used crystals, the mass sensitivity is −0.177 mg m^{-2} Hz^{-1}.[36] The energy dissipation D in QCM-D measurements is inversely proportional to the oscillating decay time constant τ of the crystal and can be calculated according to[39]

$$D = \frac{1}{\pi f \tau}$$

where τ is obtained by periodically disconnecting the oscillating crystal from the driver circuit via a computer-controlled relay during which the amplitude of the crystal oscillation decays exponentially in time. The crystals were mounted in a thermostatted liquid chamber, designed to provide a rapid, nonperturbing exchange of the liquid in contact with the active side of the sensor.

In a typical experiment, the QCM adsorption module and mounted sensor were let to stabilize with a background electrolyte solution (0.1 mM NaCl, unless stated otherwise), which was injected continuously at a flow rate of 0.12 mL/min. The constant f and D signals were offset to zero frequency and dissipation, which were then monitored for an additional 10 min to obtain the experimental baseline. Thereafter, one milliliter of freshly prepared polymer solution (0.1 μg/L concentration, in the same background electrolyte) was injected at a flow rate of 0.12 mL/min. The frequency and dissipation were monitored until constant values were reached. Following, a 3 mL buffer solution was used to rinse the adsorbed layer at the same flow rate. The system employed allowed for the measurement of up to four harmonics. In this study, the frequency and dissipation responses were recorded at ca. 15, 25, and 35 MHz, corresponding to the third, fifth, and seventh overtones (n = 3, 5, and 7, respectively). Only the normalized frequency and the dissipation shifts ($\Delta f_n/n$ and ΔD, respectively), corresponding to the third overtone ($\Delta f_3/3$ and ΔD_3), are presented in the discussion below.

It should be noted that the Sauerbrey relation does not apply to viscoelastic or soft adlayers since they may not fully couple with the motion of the sensor; i.e., the frequency change can be affected by the mechanical properties of the film, including the shear modulus and viscosity. In such cases, the Sauerbrey equation tends to underestimate the calculated mass, and therefore viscoelastic models such as that of Voigt[47−49] have been recommended. Here the viscoelastic system is conceptualized as a spring and dashpot corresponding to the elastic (storage) and inelastic (damping) behavior of the material. The energy losses (dissipation D) and the shift in frequency for the different overtones were therefore collected and fitted to the film viscosity, shear modulus, thickness, and density of the adsorbed layer using QTools software (Q-Sense). More details on this approach can be found elsewhere.[47,48]

Results and Discussion

Polyampholyte Adsorption on Silica Surfaces. ***Dynamics of Adsorption.*** We first discuss the dynamics and extent of adsorption for all polyampholytes and simple polyelectrolytes at a pH of 7 (which is close to the IEP for the amphoteric polymers), with focus on the effect of the nominal charge density of the macromolecules. In later sections, we introduce the effect of pH of the adsorbing polyelectrolyte solution on the extent of adsorption and adsorbed layer viscoelasticity. Figure 2 shows the QCM profiles corresponding to the adsorption of polyampholytes PAmp2, PAmp4, PAmp8, and PAmp16 as well as the simple polyelectrolytes "Cat" and "An" on silica at a solution pH of 7. The general features of the Δf curve as a function of adsorption time at other pH values (pH 4 and 10) followed similar trends and are not presented here for brevity.

At first, when the polymers were injected into the adsorption unit, the molecules adsorbed rapidly on the silica surface, presumably driven by net entropy gain in the system when the counterions in the polymer and the surface were released, upon adsorption. In this initial stage, all the polymers exhibited similar adsorption rates (similar slopes in the $\Delta f-t$ curves during the first seconds). Following the initial, fast adsorption, a slower adsorption dynamics was observed for the polyampholytes of higher nominal charge density (PAmp8 and PAmp16).

It was observed that the polymers carrying higher nominal charge density were adsorbed in larger amounts. In other words, they adsorbed in the form of layers that effectively reduced the resonance frequency of the sensor. This is in contrast with the behavior of simple polyelectrolytes that adsorbed on oppositely charged surfaces to a lesser extent with increased charge density.[50−52] In fact, distinctive differences in the extent and dynamics of adsorption of polyampholytes and single polyelectrolytes were observed, as shown in Figure 2.

Interestingly, the simple cationic polyelectrolyte Cat reached a (relatively small) frequency plateau much faster than any of the other adsorbing polymers. Furthermore, there was an obvious

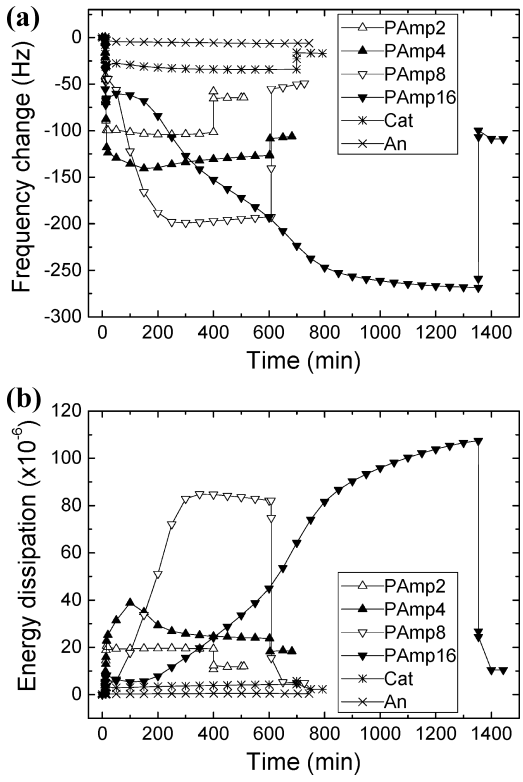

Figure 2. Changes in QCM frequency (a) and energy dissipation (b) for polyampholytes PAmp2, PAmp4, PAmp8, and PAmp16 and simple polyelectrolytes Cat and An (see Table 1) adsorbing from aqueous solution at pH 7 on silica. The different systems were rinsed with background electrolyte (polymer-free, 0.1 mM NaCl solution) solution after the respective signal became stabilized (at different times, depending on the polymer). This is indicated by a steep change in f and D.

difference between the nominal low and high charge density polyampholytes: in the first case (PAmp2 and PAmp4), a maximum adsorption was reached relatively faster with only small frequency shifts after reaching a plateau value. However, for the highly charged polyampholytes (PAmp8 and PAmp16), constant frequency was reached only after a long time. In the case of PAmp16, extremely long times, of over 20 h, were required for the frequency to become constant. It is proposed that this phenomenon is caused by slow accumulation and conformational changes of the polyampholyte at the interface. This hypothesis is also supported by observing the changes in energy dissipation (Figure 2b). The dissipation values increased with the nominal charge density of the polymers. The energy dissipation for adsorbing polyampholytes PAmp8 and PAmp16 was much larger than for polyampholytes PAmp2 and PAmp4. They were also larger than for the simple polyelectrolytes. If one takes a larger dissipation value as an indication of a thicker, softer layer, the dissipation results were therefore consistent with the formation of a highly dissipative layer.

The experiments presented in Figure 2 included a rinsing step with excess background electrolyte solutions that were effective in removing excess (loosely adsorbed) polymers from the interface. As a result, a second "plateau" frequency was reached after rinsing, and it was taken as indicative of the effective (or irreversible) amount of polymer adsorbed.

The dissipation values for all the polyampholytes were very high. For rigid, ultrathin, and evenly distributed adsorbed layers, the Sauerbrey equation describes a proportional relationship between the adsorbed mass (Δm) and the shift of the QCM crystals' resonance frequency (Δf). On the other hand, if the adsorbed material exhibits a viscoelastic behavior, such as for layers of proteins or DNA, substantial deviations from the Sauerbrey equation are expected to occur.[36,38,39,53,54] Our results fall in the latter category. Dissipation values after polyampholyte adsorption were as high as 200×10^{-6}. However, after rinsing, a sharp drop in dissipation was always observed, indicative of extensive removal of loosely bound molecules, especially in the case of PAmp8 and PAmp16.

Because the Sauerbrey approximation could not be applied for accurate calculation of the adsorbed mass, we used the Voigt model to calculate the thickness and mass of the adsorbed layers (for both polyampholytes and polyelectrolytes). The procedure for fitting the experimental data to this model is described in ref 47. In Figure 3, the thicknesses of low (PAmp2) and high (PAmp8) charge density polyampholytes are presented to illustrate how the adsorption mechanism compares in these two cases. The solid and dashed lines illustrate the thickness calculated by the Sauerbrey and the Voigt model, respectively. Even with a less dissipative adsorbed layer such as that produced by PAmp2, the Sauerbrey value was only half of the Voigt thickness. For swollen adsorbed polymer layers, such as that for PAmp8, larger differences were obtained (the Sauerbrey thickness was ca. one fourth of the Voigt value).

At pH 7 (as well as at the other values of solution pH), the surface was negatively charged since the IEP for silica is close to pH 2. Thus, it is expected that the cationic groups were responsible for the adsorption on silica, especially in the case of high charge density polyampholytes and simple polycations. It can be hypothesized that negative groups of the polyampholytes can be enriched on the side facing the bulk solution. In turn, these negative groups could interact with available cationic groups in neighboring polymers, giving rise to in further adsorption phase separation or microprecipitation close to the surface. It is worth noting that turbidity measurements did not reveal detectable changes in light transmission when any of the polymer solutions were tested (at the same concentration and solution pH and ionic strength); therefore, macroprecipitation can be ruled out in all cases. Interestingly, from Figure 3 (right) two different events occurring in the case of PAmp8 adsorption can be observed: a relatively fast adsorption (time less than 100 min) that is followed by a very slow mass buildup (reaching ca. 100 nm Voigt thicknesses). However, the extra amount of polymer that accumulated in the second phase was rinsed off rather quickly and effectively, and the residual mass after rinsing was similar to that observed at the end of the first adsorption phase (with a ca. 10 nm Voigt thickness). Therefore, it is hypothesized that the initial adsorbed layer was dense, and because of excess electrostatic charges the initial adsorbed layer was able to interact with other polyampholyte molecules in solution, thereby producing a phase separation or microprecipitation with loosely bound molecules. These observations are in striking contrast with the behavior of simple polyelectrolytes and also with polyampholytes with lower charge density, for example, PAmp2 (Figure 3, left) and PAmp4 that showed an adsorption kinetics that was quite fast, with no phase separation, as described above.

In passing, we note that changes of the solution bulk density and viscosity before and after rinsing are expected to contribute to a shift in frequency; however, this change was calculated to be small for the low polymer concentrations used in our experiments. Therefore, the observed changes are taken as the result of differences in mass in the interfacial region, next to the silica surface.

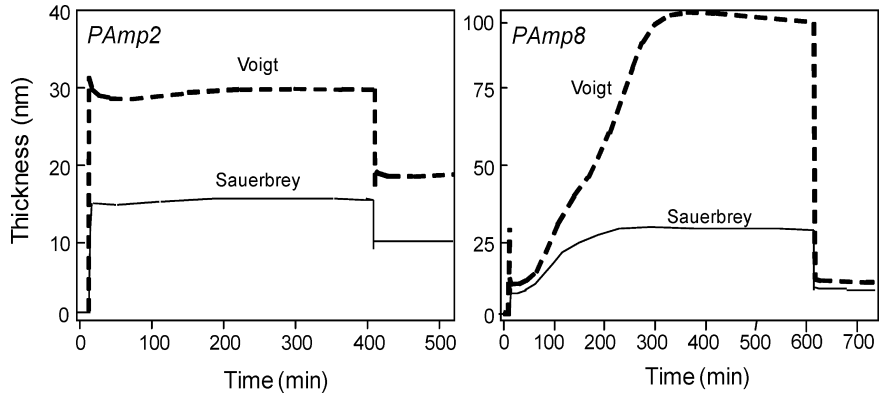

Figure 3. Comparison of adsorbed layer thickness calculated by Sauerbrey and Voigt models for polyampholytes of low (PAmp2, left) and high (PAmp8, right) nominal charge density on silica. In the left figure, PAmp2 was introduced soon after 0 min time, and rinsing with background electrolyte was performed at ca. 400 min. In the case of PAmp8 (right), rinsing was performed at ca. 600 min after injection.

Conditions of charge symmetry at neutral pH (close to the IEP) favor the contraction of the polyampholyte molecules to form globules that could accumulate at the interface. However, the same responses as described before were observed under solution conditions leading to charge asymmetry of the polyampholytes at pH 4 and 10, which favors chain expansion. Therefore, the slow changes in frequency observed upon polymer adsorption occurred regardless of the pH conditions. The existence of a phase separation or a microprecipitation zone before rinsing is therefore proposed to explain the observed changes in QCM measurements, for polyampholytes of high nominal charge density. The effect of rinsing suggests that the attraction forces between the initial, strongly adsorbed layer (formed during the first, fast phase) and neighboring macromolecules in solution (accumulated slowly during the second phase) were too weak to withstand the ensuing shear and dilution effects upon rinsing.

No simple relationship was found between the adsorbed amount after rinsing and the nominal charge density of the polyampholytes. In general, it is expected that a cationic polyelectrolyte is able to neutralize the surface charge much more efficiently than a typical polyampholyte. In the case of adsorbing polyampholytes, this neutralization process is likely to depend on the available charged groups of the macromolecule. As discussed previously, polyampholytes tend to form globules when the medium pH is close to the IEP. Therefore, the available charged groups that are able to neutralize the surface charge are highly dependent on the conformation of such structures. The net adsorption after rinsing depends not only on the charge properties of surface and those of the polyampholytes but also on the conformation of the adsorbed layers. Since polyampholytes can be expected to become reorganized under the charge-induced electrostatic fields, the net adsorption after rinsing may also depend on the dynamics of adsorption. The relationship between the initial structure of the adsorbed layer, the balance of forces, and their changes upon rinsing is a very complicated issue that deserves further investigation.

Conformation of Adsorbed Layer and Phase Separation. $\Delta D-\Delta f$ plots have been found useful in interpreting the adsorption mechanism when following the adsorption process.[36,39,53,54] The changes in slope in $\Delta D-\Delta f$ plots provide information about changes in conformational regimes of the adsorbing species. Figure 4 shows the relation between dissipation and frequency changes for polymer adsorption on silica from solution at pH 7. It is noted that for adsorption at pH 4 or 10 the $\Delta D-\Delta f$ plots exhibited similar trends: At the beginning of the adsorption process, all polymers investigated, polyampholytes and polyelectrolytes, produced a linear $\Delta D-\Delta f$ profile (see inset of Figure 4). The magnitude of the $\Delta D/\Delta f$ slope followed the same order as the nominal charge density of the polyampholytes. PAmp2 showed the steepest $\Delta D-\Delta f$ slope, indicating the buildup of a soft adsorbed layer, while the opposite was true in the case of PAmp16. This indicates that at least initially the higher charge density polyampholytes adsorb fast, as a compact layer. The cationic polyelectrolyte had a similar slope to that of PAmp16. On the other hand, the anionic polymer produced little changes in f and D (yielding only a "point" in the $D-f$ profile) due to the fact that adsorption was negligible.

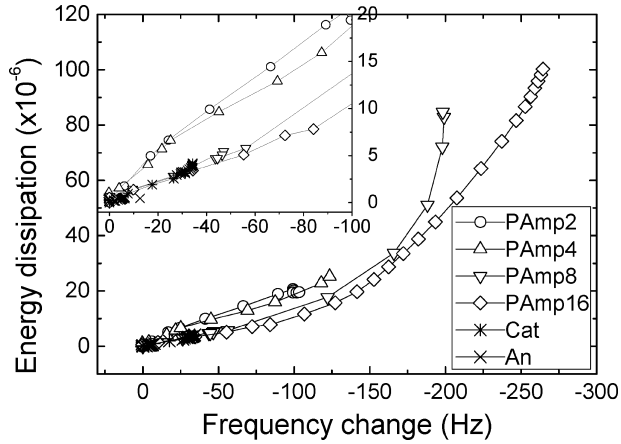

Figure 4. $\Delta D-\Delta f$ profile during adsorption on silica from aqueous solution of polyampholytes and polyelectrolytes at pH 7. Data were recorded until adsorption plateau and before applying a rinsing step.

As the adsorbed mass increased, the changes in the $\Delta D/\Delta f$ slopes differed for polyampholytes with low and high nominal charge densities. For polyampholytes with low charge density, for example, PAmp2 and PAmp4, as well as the cationic polyelectrolyte, the linear $\Delta D-\Delta f$ profile was still observed. On the other hand, polyampholytes with high charge density, for example, PAmp8 and PAmp16, showed a distinctive increase in slope with increased Δf. Before rinsing, the viscoelasticity of the adsorbed film increased extensively, and a large amount of coupled water contributed to the observed high-energy dissipation. These observations agree with our earlier discussion that a phase separation in the case of polyampholytes of high charge density took place at the interface.

Adsorption of Polyampholytes on Cellulose Thin Films. Adsorption of the studied polyampholytes on cellulose surfaces was also investigated. Figure 5 illustrates the changes in QCM

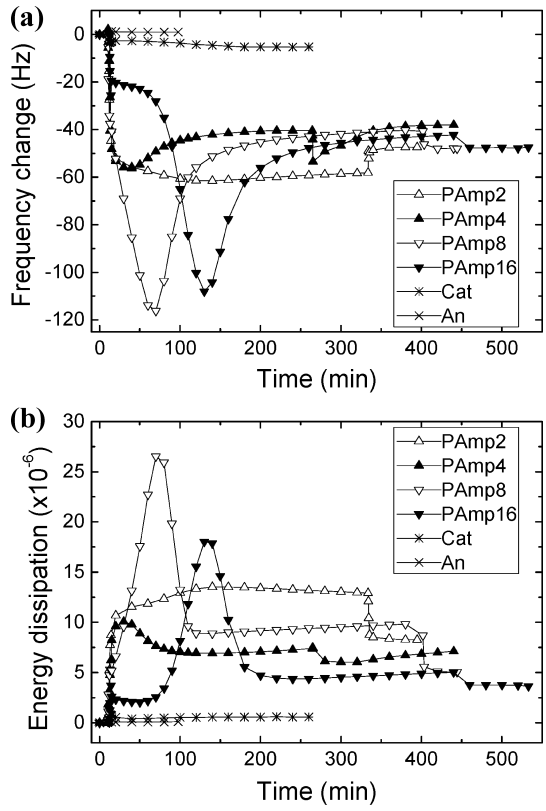

Figure 5. Changes in QCM frequency (a) and energy dissipation (b) for polyampholytes PAmp2, PAmp4, PAmp8, and PAmp16 and simple polyelectrolytes Cat and An (see Table 1) adsorbing from aqueous solution at pH 7 on thin films of cellulose.

frequency and dissipation with adsorption time after the different polymer solutions at pH 7 were contacted with cellulose.

The observed adsorption behavior was quite different from that presented for silica surfaces. These experiments were performed at least two times each, and the same trends were observed, albeit small differences in the numerical values of frequency and dissipation could be recorded. First, the extent of adsorption was much lower on cellulose compared to the case of silica surfaces. Second, for adsorption plateau the dissipation values were much higher. Additionally, frequency and dissipation curves revealed a distinctive change at some point during the adsorption process in the case of polyampholytes PAmp4, 8, and 16: A dip in QCM resonance frequency (corresponding to a maximum in energy dissipation) (see Figure 5). These changes during adsorption can also be seen in the $\Delta D-\Delta f$ profiles (not shown).

Why did layer reorganization occur distinctly in the case of cellulose substrates, as compared to silica surfaces? Several hypotheses could be suggested. A possible explanation is that after the initial, fast adsorption of the PAmp macromolecular reconformation or reorganization of the adsorbed species or the substrate occurred. Besides the difference in charge densities for silica and cellulose, it is worth noting that while the silica surface is impenetrable cellulose can be compliant and undergo additional swelling in response to events occurring around it. Because of the intrinsic nature of the cellulose, it could be argued that it may become detached from the substrate. However, extensive evidence from AFM imaging from many other experiments, conducted under severe conditions of pH and ionic strength, confirmed the robustness of the thin films of cellulose. Therefore, a likely explanation is conformational changes of the adsorbed polymer layer. Alternatively, it is

TABLE 2: Changes in Frequency and Dissipation upon Adsorption on Silica of PAmp4 from Aqueous Solution at pH Ranging from 4 to 10 (Data Recorded before Rinsing)

Δf_3 and ΔD_3 at plateau adsorption	pH solution during adsorption of PAmp4						
	4	5	6	7	8	9	10
Δf_3	−31	−71	−74	−95	−104	−92	−44
ΔD_3	5.9	18	25	33	30	22	7.8

possible that water was released from the cellulose substrate when its charges were neutralized by the adsorbing polymer, as recently shown by other authors,[55,56] and as discussed in light of the work by Kabanov et al.[57] for systems involving linear polyions and oppositely charged swollen polyelectrolyte networks.

Finally, it has recently been established that the polarization of polyampholyte chains was responsible for their adsorption on charged surfaces, resulting in the formation of multilayers.[11,58−61] Dobrynin, Rubinstein, and Joanny proposed that such a mechanism involved induced polarization of the chains in the electrostatic field extending from charged surfaces.[58] In such situations, the charge density of the surface plays an important role. Arguably, since cellulose surfaces have a lower charge density compared to that of silica surfaces,[40,62,63] it is to be expected that the conformation of adsorbed polyampholytes will be different in these cases. With increased surface charge density, different adsorption regimes (such as the pole, fence, and pancake) are expected, as proposed elsewhere.[1] The net result is the formation of a loose adsorbed layer on cellulose with little restriction to reorganization of the charged groups. However, further experiments are needed to reach definite conclusions and especially to elucidate the nature of the frequency and dissipation discontinuities shown in Figure 5.

Effect of Solution pH on Polyampholyte Adsorption. The $\Delta f-\Delta D$ profiles obtained during the adsorption of different polyampholytes in the pH range from 4 to 10 are reported below. In these experiments and compared to those reported earlier, different aqueous background electrolyte type and concentration were used (5 mM Na_2SO_4). We first present the effect of pH on the adsorption behavior of PAmp4 on silica, as can be observed in Table 2.

The data in Table 2 do not reveal the time required for PAmp4 to reach the plateau adsorption; however, we point out that in neutral pH such a condition was reached after significantly longer times, as compared to adsorption from solution at either lower or higher pH values. The IEP for PAmp16 was 7.3 at an ionic strength of 10 mM salt concentration. Similar values of IEP apply to the other polymers (PAmp2, 4, and 8). It is around this neutral pH value where the maximum change both in frequency and in dissipation was observed. As the pH of the adsorbing solution departed from the IEP values (pH increased toward pH 10 or reduced to pH 4), a reduction in the plateau frequency and dissipation was apparent.

Figure 6 summarizes the adsorption behaviors, as a function of solution pH (4, 7, and 10), for three representatives of the polymers studied: The simple cationic polyelectrolyte (Cat), a low charge density polyampholyte (PAmp4), and the polyampholyte with the highest charge density (Pamp16). If one takes a larger frequency as an indication of a larger adsorbed amount, it is clear that in all cases the extent of adsorption for polyampholytes was consistently larger than for those of simple polyelectrolytes. For the negatively charged polyelectrolyte, An, negligible adsorption occurred. In the case of the polyampholytes, it is evident that changes in the pH of the polymer solution played a distinctive role in terms of the extent of polyampholyte adsorption. Dobrynin and Rubinstein[58] demon-

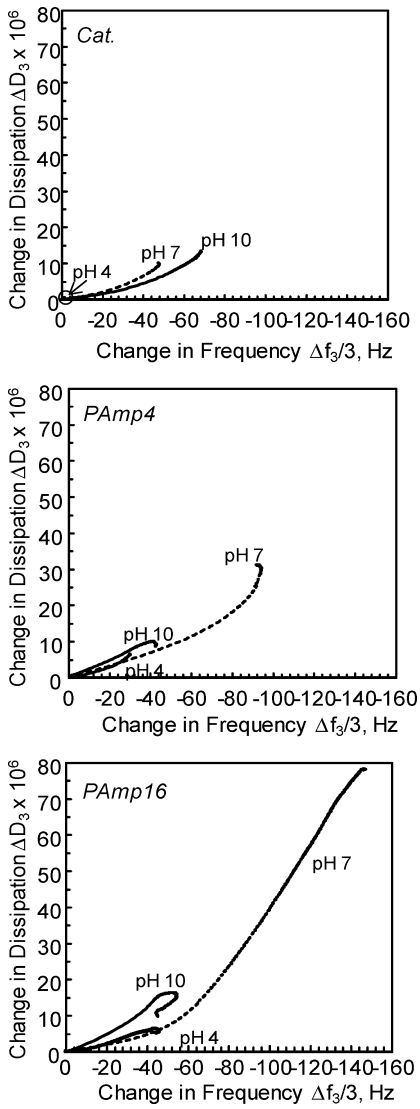

Figure 6. $\Delta D-\Delta f$ profiles obtained during the adsorption of the cationic polyelectrolyte and polyampholytes PAmp4 and PAmp16 on silica from aqueous solution at pH 4, 7, and 10.

strated that because of the anionic and cationic groups in polyampholytes they are able to adsorb on both cationic and anionic surfaces. In our case, we used silica, which is negatively charged at all pH values used in these experiments. We expect that depending on the pH of the adsorbing solution the adsorbed polymers could change conformation to allow their opposite charge groups to interact more effectively with the charged surfaces. Also, nonionic interactions between acrylamide segments of the polymers and silica are expected to contribute to adsorption. However, decoupling the electrostatic and nonelectrostatic contributions to explain the observed behavior is rather challenging. Some light can be shed by performing experiments at different ionic strengths, and this is the subject of a forthcoming report.

In the case of the adsorption of Cat, we observed that at pH 4 a negligible amount was adsorbed on silica, whereas the extent of adsorption increased with increases of the solution's pH. This is easily explained by the fact that at higher pH the charge density of the silica surface increases. For example, Durval et al. studied the surface composition of a quartz surface reacted with aqueous solutions with pH ranging from 0 to 10. By using X-ray photoelectron spectroscopy, they determined the presence of three surface species, $SiOH_2^+$, $SiOH^0$, and SiO^-, the composition of which varied depending on the pH. Furthermore, the density of the silanol group (SiO^-) increased significantly with pH, while a higher proportion of positive charged $SiOH^{2+}$ groups were found at extremely acidic conditions. At pH 6, the dominant species was $SiOH^0$.[64]

These observations, however, do not explain the extent of adsorption of the polyampholytes at the various pH values tested: Polyampholyte adsorption did not reach a maximum at the highest pH but at an intermediate pH of 7, i.e., under conditions of polyampholytes' charge symmetry. This fact indicates that it is not the charge density of the substrate but rather some other reason for the observation of a maximum adsorption at neutral pH (for both PAmp4 and PAmp16). Polyampholytes with high charge asymmetry (at pH 4 and pH 10, which are conditions far from the IEP of the polyampholytes) tend to be extended, while at pH 7, which is very close to their IEP, they tend to contract into globules; it can be recalled that the radius of gyration of PAmp4 in aqueous solution at pH 7 was ca. 69 nm, while at pH 4 and pH 10 it was 95 and 182 nm, respectively. The conformation of the same polyampholytes in solution (extension or contraction according to the pH conditions) and the resulting solution viscosity were correlated in earlier reports by the authors.[20] All in all, at pH 7 the polyampholytes are in the globular form, with a (close to) minimum radius of gyration. In such circumstances, the initial monolayer of adsorbing macromolecules can fit optimally on the surface. It is also in this condition of charge symmetry that the inductive influence of neighboring groups promotes the buildup of a large adsorbed amount. A maximum adsorption at around the IEP has also been reported for natural polyampholytes.[65] The dissipation in this case is largest, which means that the adsorbed layers are highly hydrated and energy dissipative. In the case of other polyampholytes, for example, PAmp16, similar conclusions can be drawn. However, as noticed earlier in the discussion about the effect of polyampholytes nominal charge density, phase separation or microprecipitation gave rise to even larger changes in frequency and dissipation.

Figure 7 illustrates qualitatively the balance of electrostatic charges between silica and the studied polymers. The silica surface is negatively charged within the pH range from 4 to 10, while the simple cationic and anionic polyelectrolytes are always positively and negatively charged, respectively. Conditions for polyampholytes charge asymmetry occur between pH 4 and the respective IEP (net positive charges), while a net negative charge is dominant between the respective IEP and pH 10.

The polyampholytes carry net negative charges at pH 10. If one were to consider only the net charge, then it might be expected that no or little polyampholyte adsorption would occur at high pH, where silica is also negatively charged. This is in contrast with our experimental observations since there was a sizable adsorption at this pH. This effect can be explained by the effect of polarization of the polyampholyte chains in the external electrostatic field created by the charged silica substrate. The formation of hydrogen bonding between the polymers and the surfaces in these cases could also be a contributing factor.

Khan et al. used mean-field and Monte Carlo simulations to conclude that for large enough surface charge densities adsorption of polyampholytes occurred under conditions of polymer charge balance or when carrying the same net charge as the surfaces.[66] Likewise, Mahltig el al.[67] reported experiments on the adsorption of diblock polyampholytes which occurred even when the substrate and the polyampholytes exhibited the same sign of net charge. They also found maximum adsorbed amounts

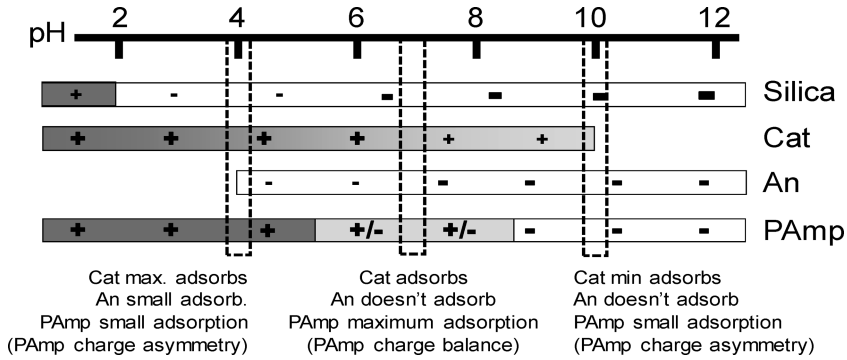

Figure 7. Illustrative chart with the net charge of surfaces and polymers at different pH and indication of dominant adsorption effect at pH 4, 7, and 10.

close to the IEP of the polymer as a function of pH; however, directly at the IEP of the polyampholyte, no adsorption was measurable. This behavior was explained by the fact that a similar IEP of polymer and substrate were used. Under these conditions, the surface charge density was close to zero, and therefore electrostatic interactions were limited. This example underscores the importance of the charge balance (polyampholytes charge asymmetry and surface charge density), as pointed out in Figure 7.

In summary, it is apparent that considerably greater adsorption took place at neutral pH, compared to higher or lower pH values. These results are consistent with the following anticipated effects of pH on the charged natures of both the polyampholyte and the silica substrate. A low pH of 4 is expected to increase the net cationic charge of the polyampholyte since pH 4 is below the apparent pK_a value of at least one of the carboxylic acid groups in each monomer group derived from itaconic acid.[68] At the same time, the negative charge of the substrate is expected to be substantially less at pH 4, compared to neutral pH. On the basis of the charge asymmetry of the polyampholyte and the charge density of the substrate, therefore, the adsorption at the lower pH is expected to be less. A somewhat different argument is needed to explain the effects at pH 10. In that case, although the silica substrate is expected to have a strong negative charge, the pH is high enough so that a substantial proportion of the amine groups on the polyampholyte will be in their deprotonated, neutral form, thus reducing the number of positive groups, at any moment of time, that are available to engage in complexation interactions with the negatively charged substrate.

In an attempt to corroborate the points just made, PAmp4 and PAmp16 were compared on the basis that they have the same ratio of positive to negative groups but with four times higher molar content of each type of charged monomer in the case of PAmp16. From the respective results, the relative positions of the curves were similar for both cases, and the net adsorption of the polyampholyte having higher density of chargeable groups appeared to be considerably higher under neutral pH conditions. The dissipation data indicate that such apparent greater adsorption may have been due to a higher content of water held within the adsorbed layer in this case.

Numerical simulations by other groups have shed light on the adsorption behavior of polyampholytes on charged surfaces. This in part has been done with the aim to better understand protein adsorption. Our experimental results highlight the importance of the balance of charges. Finally, since the charge sequence along the polymer backbone plays an important role in the solution and adsorbing properties, an important distinction has to be made regarding the application of our results to biomacromolecules. Contrary to the case of synthetic polyampholytes with random charge distribution, proteins are expected to contain amino acid sequences leading to unique three-dimensional structures or conformations. The effect of salt addition on the screening of the electrostatic interactions between unbalanced charges is expected to play an important role which will be highlighted in a future communication.

Conclusions

The adsorption onto charged surfaces by four polyampholytes, all having a fixed charge ratio of 5:4 cationic to anionic and with increasing content of ionizable groups in the ratios of 1:2:4:8, as well as two simple polyelectrolytes (anionic and cationic), were measured by using the QCM-D technique. It was found that the charge properties of both substrates and polymers were crucial in determining the adsorption mechanism, the extent of adsorption, and the molecular conformations. Fast, initial absorption in the case of high charge density surfaces and polyampholytes with high nominal charge density was driven by electrostatic mechanisms. Under this situation, however, macromolecule accumulation, possibly microprecipitation or phase separation near the interface, was detectable with quartz crystal microgravimetry. For surfaces of low charge density adsorbing polyampholytes of low nominal charge density, electrostatic and polarization effects were minimized. Under this situation, simple, more compact layers were observed. Overall, the results presented in this report allow a better understanding of polyampholyte adsorption and reveal that the extension of adsorption and conformation of the adsorbed species is a result of a subtle balance of factors, including charge properties of surfaces, charge density of polyampholytes, and the polymer charge asymmetry, which is affected by the pH of the aqueous medium.

Acknowledgment. The authors would like to acknowledge funding support from the USDA Cooperative State Research, Education and Extension Service, grant number 2004-35504-14655. Dr. T. Sezaki (Harima Chemical Corp., Japan) is gratefully acknowledged for synthesizing and providing the polyampholyte and polyelectrolyte samples.

Note Added after ASAP Publication. This paper was published ASAP on November 19, 2009. Due to production error, data in Table 1 was displaced. The revised paper was reposted on November 23, 2009.

References and Notes

(1) Dobrynin, A. V.; Colby, R. H.; Rubinstein, M. *J. Polym. Sci., Part B* **2004**, *42*, 3513.
(2) Ertas, D.; Kantor, Y. *Phys. Rev. E* **1996**, *53*, 846.

(3) Gutin, A. M.; Shakhnovich, E. I. *Phys. Rev. E* **1994**, *50*, R3322.
(4) Hwang, D. C.; Damodaran, S. *J. Appi. Polym. Sci.* **1996**, *62*, 1285.
(5) Jeon, J.; Dobrynin, A. V. *Macromolecules* **2005**, *38*, 5300.
(6) Kantor, Y.; Kardar, M. *Phys. Rev. E* **1995**, *51*, 1299.
(7) Lee, N.; Thirumalai, D. *J. Chem. Phys.* **2000**, *113*, 5126.
(8) Long, D.; Dobrynin, A. V.; Rubinstein, M.; Ajdari, A. *J. Chem. Phys.* **1998**, *108*, 1234.
(9) Lord, M. S.; Stenzel, M. H.; Simmons, A.; Milthorpe, B. K. *Biomaterials* **2006**, *27*, 567.
(10) Yamakov, V.; Milchev, A.; Limbach, H. J.; Dunweg, B.; Everaers, R. *Phys. Rev. Lett.* **2000**, *85*, 4305.
(11) Dobrynin, A. V. *Phys. Rev. E* **2001**, 6305.
(12) Anderson, N. J.; Bolto, B. A.; Eldridge, R. J.; Jackson, M. B. *React. Polym.* **1993**, *19*, 87.
(13) Kudaibergenov, S. E.; Ciferri, *Macromol. Rapid Commun.* **2007**, *28*, 1969.
(14) Wang, Y.; Hubbe, M. A.; Rojas, O. J.; Argyropoulos, D. S.; Wang, X.; Sezaki, T. *Colloids Surf., A* **2007**, *301*, 33.
(15) Silva, D. J.; Rojas, O. J.; Hubbe, M. A.; Park, S. W.; Yamaguchi, T.; Song, O. P. **2009**, in press.
(16) Ozon, F.; di Meglio, J. M.; Joanny, J. F. *Eur. Phys. J. E* **2002**, *8*, 321.
(17) Carr, M. E.; Hofreiter, B. T.; Schulte, M. I.; Russell, C. R. *Tappi J.* **1977**, *60*, 66.
(18) Hubbe, M. A.; Rojas, O. J.; Argyropoulos, D. S.; Wang, Y.; Song, J.; Sulic, N.; Sezaki, T. *Colloids Surf., A* **2007**, *301*, 23.
(19) Hubbe, M. A.; Rojas, O. J.; Sulic, N.; Sezaki, T. *Appita J.* **2007**, *60*, 106.
(20) Song, J.; Wang, Y.; Hubbe, M. A.; Rojas, O. J.; Sulic, N.; Sezaki, T. *J. Pulp Pap. Sci.* **2006**, *32*, 156.
(21) Alfrey, T., Jr.; Morawetz, H.; Fitzgerald, E. B.; Fuoss, R. M. *J. Am. Chem. Soc.* **1950**, 1864.
(22) Bratko, D.; Chakraborty, A. K. *J. Phys. Chem.* **1996**, *100*, 1164.
(23) Kantor, Y.; Kardar, M.; Li, H. *Phys. Rev. E* **1994**, *49*, 1383.
(24) Schiessel, H.; Blumen, A. *J. Chem. Phys.* **1996**, *104*, 6036.
(25) Schiessel, H.; Blumen, A. *J. Chem. Phys.* **1996**, *105*, 4250.
(26) Srivastava, D.; Muthukumar, M. *Macromolecules* **1996**, *29*, 2324.
(27) Tran, Y.; Perrin, P.; Deroo, S.; Lafuma, F. *Langmuir* **2006**, *22*, 7543.
(28) Huguenard, C.; Varoqui, R.; Pefferkorn, E. *Macromolecules* **1991**, *24*, 2226.
(29) Billingham, J.; Breen, C.; Yarwood, J. *Vib. Spectrosc.* **1997**, *14*, 19.
(30) Zalczer, G.; Gurfein, V. *Macromolecules* **1992**, *25*, 2634.
(31) Durbruel, P.; Urtti, A.; Schacht, E. *Macromol. Rapid Commun.* **2005**, *26*, 992.
(32) Green, R. J.; Davies, J.; Davies, M. C.; Roberts, C. J.; Tendler, S. J. *Biomaterials* **1997**, *18*, 405.
(33) Sarkar, D.; Somasundaran, P. *Langmuir* **2004**, *20*, 4657.
(34) Toyama, S.; Aoki, K. *Chem. Sensors* **2003**, *19*, 46.
(35) Toyama, S.; Aoki, K.; Kato, S. *Chem. Sensors* **2004**, *20*, 542.
(36) Edvardsson, M.; Rodahl, M.; Kasemo, B.; Hook, F. *Anal. Chem.* **2005**, *77*, 4918.
(37) Marx, K. A.; Zhou, T.; Sarma, R. *Biotechnol. Prog.* **1999**, *15*, 522.
(38) Rodahl, M.; Kasemo, B. *Sens. Actuators, B* **1996**, *37*, 111.
(39) Rodahl, M.; Kasemo, B. *Sens. Actuators, A* **1996**, *54*, 448.
(40) Radtchenko, I. L. P. G.; Borkovec, M. *Biomacromolecules* **2005**, *6*, 3057.
(41) Falt, S.; Wågberg, L.; Vesterlind, E. L.; Larsson, P. T. *Cellulose* **2004**, *11*, 151.
(42) Gunnars, S.; Wågberg, L.; Stuart, M. A. C. *Cellulose* **2002**, *9*, 239.
(43) Song, J.; Liu, X.; Liang, J.; Krause, W. E.; Hinestroza, J. P.; Rojas, O. J. *Solid Thin Films* **2009**, *17*, 4348.
(44) Notley, S. M.; Pettersson, B.; Wågberg, L. *J. Am. Chem. Soc.* **2004**, *126*, 13930.
(45) Notley, S. M.; Wagberg, L. *Biomacromolecules* **2005**, *6*, 1586.
(46) Sauerbrey, G. *Z. Phys.* **1959**, *155*, 206.
(47) Voinova, M. V.; Rodahl, M.; Jonson, M.; Kasemo, B. *Phys. Scr.* **1999**, *59*, 391.
(48) Stengel, G.; Höök, F.; Knoll, W. *Anal. Chem.* **2005**, *77*, 3709.
(49) Garg, A.; Heflin, J. R.; Gibson, H. W.; Davis, R. M. *Langmuir* **2008**, *24*, 10887.
(50) Durand-Piana, G.; Lafuma, F.; Audebert, R. *J. Colloid Interface Sci.* **1987**, *119*, 474.
(51) Denoyel, R.; Durand, G.; Lafuma, F.; Audebert, R. *J. Colloid Interface Sci.* **1990**, *139*, 281.
(52) Rojas, O. J.; Ernstsson, M.; Neuman, R. D.; Claesson, P. M. *Langmuir* **2002**, *18*, 1604.
(53) Hook, F.; Kasemo, B.; Nylander, T.; Fant, C.; Sott, K.; Elwing, H. *Anal. Chem.* **2001**, *73*, 5796.
(54) Su, X. D.; Zong, Y.; Richter, R.; Knoll, W. *J. Colloid Interface Sci.* **2005**, *287*, 35.
(55) Notley, S. M. *Phys. Chem. Chem. Phys.* **2008**, *10*, 1819.
(56) Enarsson, L.-E.; Wågberg, L. *Biomacromolecules* **2009**, *10*, 134.
(57) Kabanov, V. A.; Zezin, A. B.; Rogacheva, V. B.; Prevish, V. A. *Makromol. Chem.* **1989**, *190*, 2211.
(58) Dobrynin, A. V.; Rubinstein, M.; Joanny, J. F. *Macromolecules* **1997**, *30*, 4332.
(59) Dobrynin, A. V.; Obukhov, S. P.; Rubinstein, M. *Macromolecules* **1999**, *32*, 5689.
(60) Zhulina, E.; Dobrynin, A. V.; Rubinstein, M. *Eur. Phys. J. E* **2001**, *5*, 41.
(61) Zhulina, E. B.; Dobrynin, A. V.; Rubinstein, M. *Eur. Phys. J. B* **2001**, *105*, 8917.
(62) Poptoshev, E.; Claesson, P. M. *Langmuir* **2002**, *18*, 2590.
(63) Poptoshev, E.; Claesson, P. M. *Langmuir* **2002**, *18*, 1184.
(64) Duval, Y.; Mielczarski, J. A.; Pokrovsky, O. S.; Mielczarski, E.; Ehrhardt, J. J. *J. Phys. Chem. B* **2002**, *106*, 2937.
(65) Curme, H. G.; Natale, C. C. *J. Phys. Chem. B* **1964**, *68*, 3009.
(66) Khan, M. O.; Åkesson, T.; Jonsson, B. *Macromolecules* **2001**, *34*, 4216.
(67) Mahltig, B.; Walter, H.; Harrats, C.; Muller-Buschbaum, P.; Jerome, R.; Stamm, M. *Phys. Chem. Chem. Phys.* **1999**, *1*, 3853.
(68) Wang, Y.; Hubbe, M. A.; Sezaki, T.; Wang, X. W.; Rojas, O. J.; Argyropoulos, D. S. *Nordic Pulp Pap. Res. J.* **2006**, *21*, 638.

JP909047T